In: Explosive Materials Classification, Composition & Properties ISBN 978-1-61761-188-9
Editor: Thomas J. Janssen, pp. 125-144

Chapter 5

THERMAL METHODS OF ANALYSIS AS A TOOL FOR QUANTITATIVE COMPOSITION DETERMINATION OF "WATER-IN-OIL" EMULSIONS

Romana Cerc Korošec [*] ***and Peter Bukovec***
Faculty of Chemistry and Chemical Techology, University of Ljubljana,
Aškerčeva 5, SI-1000 Ljubljana, Slovenia

ABSTRACT

Thermal methods of analysis, especially thermogravimetry (TG) and differential scanning calorimetry (DSC), are often applied for determination of thermal properties of different types of explosive materials (e.g., thermal stability, thermal decomposition characteristics and kinetics of decomposition process) and also for identification of an unknown explosive (on the basis of an established database). On the other hand, due to several factors which influence the outcoming signal, these methods seem less suitable for quantitative analysis of explosives.

The main component of an emulsion explosive is water-in-oil emulsion consisting of a supersaturated ammonium nitrate (AN) water phase, finely dispersed in an oil phase. Quantitative determination of a single component in an emulsion can be time consuming, but a reasonable combination of both above-mentioned thermal methods proved to be suitable for quantitative determination of nearly all the components in an emulsion. Isothermal TG measurements enable determination of water content, while successive heating and cooling DSC measurements allow the amount of AN to be determined. In the case that sodium nitrate (SN) is also added to AN as an oxidizing agent, it is necessary to quantitatively separate both salts from organic matter with diethyl ether. On the basis of the dynamic TG curve of the precipitated salts, the amount of AN can then be calculated, and that of SN is obtained from dynamic TG measurement of the original sample. Unknown ratio between AN/SN in an emulsion was also determined from the liquidus curve of the binary phase diagram, a part of which was constructed for this purpose. In that case, separation from organic matter was not necessary.

[*] E-mail: romana.cerc-korosec@fkkt.uni-lj.si

1. INTRODUCTION

1.1.Thermal Methods

Thermal analysis (TA) is defined by the International Confederation for Thermal Analysis and Calorimetry (ICTAC) and means the analysis of a change in a sample property, which is related to an imposed temperature alteration [1]. This definition includes heating or cooling process, isothermal temperature programs as well as modulation modes, where additional change in temperature with constant frequency and amplitude is superposed on a linear heating or cooling ramp. By property of the sample thermodynamic properties (temperature, heat, enthalpy, mass, volume,…), material properties (hardness, Young´s modulus,…), chemical composition or structure is meant, and therefore the number of different thermal methods is large. The most common methods used are thermogravimetry (TG), differential thermal analysis (DTA), differential scanning calorimetry (DSC), thermomechanical analysis (TMA) and evolved gas analysis (EGA). In many cases the use of one single TA technique may not provide sufficient information about the process or reaction. Then complementary or supplementary information may be required by other thermal analysis techniques or by *ex-situ* measurements of intermediates, taken during the thermal process or of the final residue. A comprehensive practical overview on most commonly used methods, instrumentation, factors affecting the obtained curves and selected examples from inorganic chemistry is given in [2].

Thermogravimetry is a technique where the change in sample mass (mass loss or gain) is measured as a function of temperature and/or time. In dynamic measurements the sample is heated in an environment whose temperature is linearly increasing, whereas in isothermal measurements the sample mass is recorded as a function of time at constant temperature. In quasi-isothermal mode the sample is heated to constant mass at each of a series of increasing temperature. Except for the mass changes, the shape of thermogravimetric curve corresponding to the course of the thermal decomposition of a substance depends on several instrumental (heating rate, type of the atmosphere used, geometry of sample holder and furnace, material of sample holder) and sample parameters (sample mass, particle size, sample packing, heat of reaction,…). Prior to TG studies, mass and temperature calibrations are required. A standard reference material is used for mass calibration and this material is checked against a pre-calibrated microbalance having a reproducibility of ± 1 μg. In modern instruments standard weights are already built-in in the instrument and mass calibration is automatically made. For temperature calibration a Curie point technique is used in vertically positioned furnaces [3]. Chosen ferromagnetic sample is placed in a sample holder and an external magnetic field is applied to the sample. The sample is then heated with a predetermined temperature program. At a defined temperature (Curie temperature) the sample becomes paramagnetic, causing apparent mass change at this transition. Calibration with pure metals is much more accurate [4] and can be easily performed in vertically positioned furnaces, in which a thermocouple is placed below the sample holder.

For accurate measurements of the sample mass in non-evacuated atmosphere, a corresponding thermogravimetric curve obtained for an empty crucible (a baseline) should be measured before the investigated sample. The sample holder floats in the atmosphere with a certain density. Any changes in its density cause change in buoyancy and in the measured

resultant weight (Figure 1). At the beginning of dynamic measurements, the density of the gas phase decreases, resulting in a slight apparent weight gain. At higher temperatures atmospheric turbulence becomes pronounced, leading to a contra effect, i.e., weight loss. Apparent weight is corrected by subtraction of an adequate baseline, which is measured with the holder of the same size, the same temperature program, the same gasses and flow rates as the sample afterwards. Subtraction of the baseline is nowadays performed automatically.

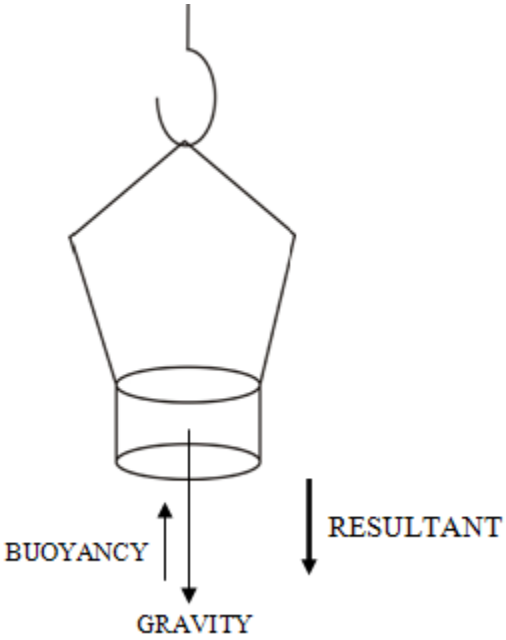

Figure 1. Forces in thermogravimetrc measurements, which influence the measured quantity, weight.

Thermoanalytical technique called differential scanning calorimetry (DSC) concerns the measurement of energy changes in a sample. Sample and inert reference material are both subjected to predetermined temperature programme. During the measurement a difference in a heat flow between the sample and a reference is monitored while the temperature difference between both is kept at zero. Temperatures of thermally induced processes (melting, sublimation, vaporization, dehydration, thermal decomposition, oxidation and reduction and changes in crystalline structure) and quantitative determination of endothermic or exothermic enthalpy changes of these processes are determined by DSC. In a similar technique, differential thermal analysis (DTA), a temperature difference between the sample and a reference material is measured as a function of temperature or time, and provides mainly equivalent information as DSC. However, DSC is preferred for quantitative heat flow measurements. As in thermogravimetry, the operational parameters (sample and particle size, heating rate,…) influence the DSC curve. Temperature and enthalpy calibration is based on the melting process of high-purity metals.

Evolved gas analysis, defined by ICTAC Nomenclature Committee, is “a technique of determining the nature and amount of volatile products or products formed during thermal analysis” [5]. This definition includes coupled techniques such as TG-MS (Thermogravimetry-Mass Spectrometry), TG-FTIR (Fourier Transform Infra Red) and also

TPR (Temperature Programmed Reduction) and TPD (Temperature Programmed Desorption) coupled to a detection system, and all other techniques by which gases are released and detected either directly or indirectly by using a solvent or an adsorbent [6]. The advantage of mass spectroscopy is the ability to detect all gaseous species at very high sensitivity.

1.2. Emulsion Explosives

Emulsion explosives possess several advantages in comparison with traditional nitroglycerine based dynamites. Their excellent properties like unusually high rates of detonation, which enable them to create fractures in rock, their good safety properties (resistance to handling, immunity to changes in temperature) and low basic cost contributed to their becoming widespread after their development in 1962 [7, 8].

The main component of an emulsion explosive is water-in-oil emulsion, where a highly supersaturated water salt solution with a droplet size of around 1 μm is finely dispersed in a small volume of hydrocarbon oil, which forms a thin film around the droplets. The water phase generally contains ammonium nitrate (AN) and other salts, such as sodium (SN) and calcium nitrate, and is metastable due to supersaturation. Ammonium nitrate is the cheapest source of oxygen available in condensed form for commercial explosives. It is the major ingredient of the emulsion, about 70 % of the overall composition. The dispersed aqueous phase, which constitutes over 90 weight % of the liquid fraction, is emulsified in 7 to 10 % of oil phase. The emulsifier (1 to 2 wt. %) enables formation and stabilization of the emulsion comprising the two phases with very different polarity, and also maintains the supercooled state. The film separating the droplets may be extremely thin – down to 3 nm [7]. In Figure 2 a schematic model of water in oil emulsion is presented.

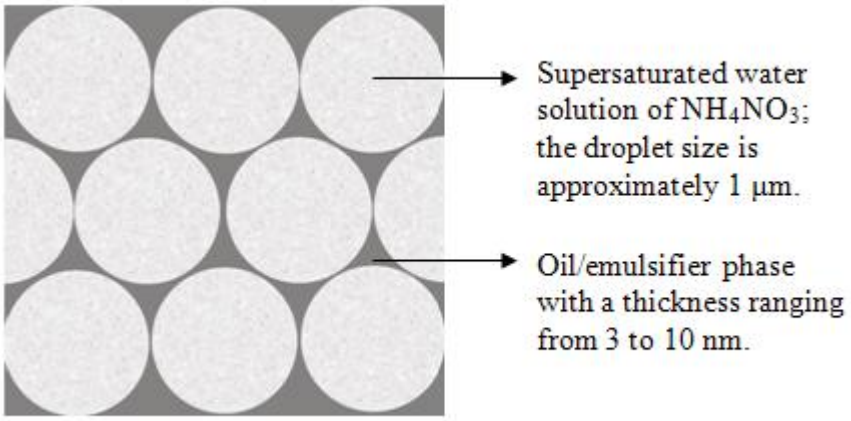

Figure 2. Schematic model representing emulsion composition.

The emulsion in not yet an explosive. An effective commercial explosive is obtained when glass or plastic microbubbles, which lower the density of the system, and optionally metal particles like aluminum powder as high energy fuel, is added to such an emulsion. The

preparation of an explosive can be done on site in a mobile unit before pumping the final emulsion into the drilled hole [7]. The type and distribution of the bubbles is critical in determining the detonation performance of the emulsion explosive. Water proves to be an effective detonation inhibitor, and the desired sensitivities are achieved by controlling water levels in the formulation. On the other hand, diminishing water content, which can occur due to its evaporation during storage, can cause crystallization in the supersaturated water phase. Stability requirements are particularly demanding for these emulsions since crystallization, particle growth or emulsion breakdown causes the loss of the required explosive properties [7].

1.3. Scope of the Work

Among various measuring techniques, TG and DSC as complementary methods of thermal analysis play important role in the analysis of explosive materials. A variety of studies was made on determination of their thermal properties (melting process, polymorphic transformation, decomposition behavior, thermal stability) [9-14], decomposition kinetics [15-18], purity determination [19, 20], heat capacity [21], study of compatibility [17, 22-24] and also for hazard evaluation of pyrotechnics [25]. Thermal methods of analysis were also used for quantitative purposes like determination of phlegmatiser content, for identification and determination of impurities and volatile compounds [20]. However, due to several reasons which affect the accuracy and reproducibility of the obtained values, these methods were seldom applied for quantitative analysis of explosive materials [20]. The sample heterogeneity and the associated problem of small sample size used for analysis on the one hand and, on the other, the dynamic character of events taking place during measurement, which is expressed through the influence of the mass of the sample and the heating rate on the outcoming signal, may all affect the precision of quantitative analysis. These factors explain why the derivation of truly quantitative data requires precise calibration, taking into account all the necessary corrections.

Complex composition of modern explosive materials demands good analytical technology, which is available to identify any explosive material. But the vast range of chemical compounds that can be encountered is such that no single analytical procedure can identify all the individual components. A systematic approach utilizing a combination of various methods is generally necessary and the investigation of slurry explosives can be rather time consuming [26]. This paper is a continuation of our previous study, where we have introduced a combination of both thermal methods, TG and DSC, for quantitative determination of water, ammonium and sodium nitrate contents in an emulsion formulation [27]. This approach demands a minimum of analytical work, such as for instance separation of a single phase and aims to minimize the errors arising from that. Accurate and precise results on quantitative composition of emulsion are needed for quality control, and also for determining its stability (water content, crystallization of AN) during its shelf-life.

2. EXPERIMENTAL

Ammonium nitrate 99.999 % (AN standard) and sodium nitrate (99.999 %) from Sigma – Aldrich was used. Before each measurement AN was dried for several hours at 150 ^{o}C. Two commercial samples, used in the area of Slovenia, were analyzed. Both are "water-in-oil" emulsions; in sample 1 AN is the sole oxidizing agent, whereas in sample 2 also some SN is added.

The morphology of the sample 1 was investigated with scanning electron microscope (SEM, Supra 35LV). Sample was simply put on a conducting carbon tape.

Thermogravimetric measurements were performed on a Mettler Toledo TG/SDTA 851^{e} instrument in a dynamic air atmosphere with a flow rate of 100 mL min^{-1}. In dynamic measurements about 20 –30 mg of the sample 1 or 2 was weighed in a 150 μL alumina crucible and cover with a pierced lid. The heating rate was 5 K min^{-1} within the temperature range from 25 up to 850 °C. The baseline was subtracted.

The maximal resolution method ("max res") was carried out over a temperature range from 25 up to 300 °C. The parameters in the max res method were set as follows: maximal heating rate 2 K min^{-1}, minimal heating rate 0.5 K min^{-1}, high threshold 0.2 μg s^{-1}, and low threshold 0.05 μg s^{-1}. That means when the weight loss exceeded 0.2 μg s^{-1}, the heating rate was automatically lowered to 0.5 K min^{-1}. An aluminum crucible, covered with a 50 μL perforated lid, was used in this experiment. Since the temperature programme is not known before the "max res" measurement, a baseline could not be subtracted. Isothermal measurements at 100 ^{o}C were performed in a 40 μL Al pan, covered with a 50 μm perforated lid. The furnace was heated at a heating rate of 5 K min^{-1} from 25 up to 100 ^{o}C and than held at isothermal temperature for 6 hours. The baseline was subtracted.

EGA measurements were performed on STA 409 Netzsch apparatus. Evolved gases were detected using a Leybold Heraeus Quadrex 200 mass spectrometer. 13.11 mg of the sample was weighed into 100 μL alumina crucible and covered with a pierced lid. During the measurement the furnace was purged with air (flow rate 100 mL min^{-1}). The heating rate was 5 K min^{-1}.

DSC analysis was carried out using a Mettler Toledo DSC 822^{e} under the same atmosphere as TG measurements. Examined samples (mass around 4 mg) were weighed in a 40 μL Al pan. Several heating and cooling cycles within the temperature range from 25 to 135°C at a rate of 5 K min^{-1} were performed on the AN standard, and samples 1 and 2. In the repeated cycles sometimes open crucibles were used, or they were covered with a pierced lid, and in a third case with 50 μm perforated lid. As a reference an empty pan was used, covered in the same manner as the sample pan. The DSC analyzer was calibrated with high purity gallium, indium and zinc. Gallium was supplied by Physikalisch-Technische Bundesanstalt Braunschweig, whereas zinc and indium came from Mettler Toledo. DSC standards and all samples for DSC analysis were carefully weighed on a Mettler Toledo MX5 balance.

For sample 2, separation of AN and SN from the emulsion was made. An aliquot of the sample was mixed with diethyl ether by rotation. Both salts are insoluble in diethyl ether, while oil and emulsifier remained in solution. After precipitation the salts were filtered. The precipitate was dried at 70 °C.

DSC measurements used for construction of a part of AN/NN phase diagram were performed with a heating rate of 2 K min^{-1}.A temperature range was from 25 to 150 ^{o}C or to 170 ^{o}C. 40 μL aluminum crucibles, covered with a pierced lid, were used.

3. RESULTS AND DISCUSSION

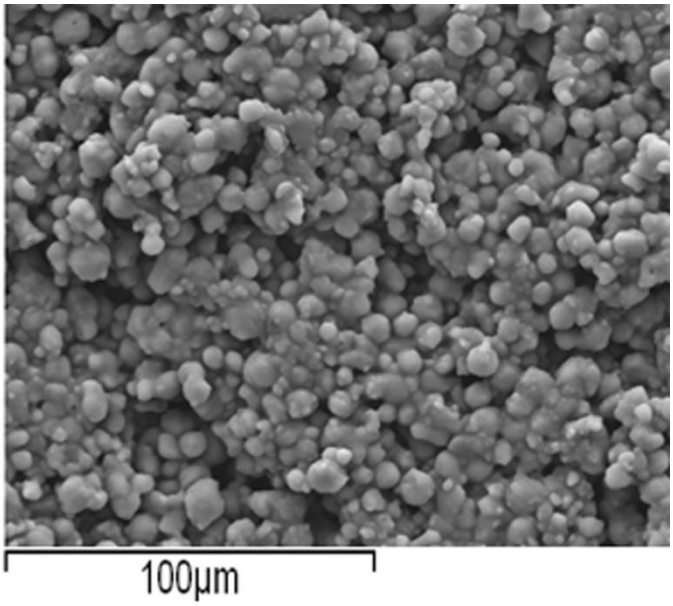

Figure 3. SEM micrograph of the sample 1.

Figure 3 represents a SEM image of sample 1. The size of the spherical particles, which are droplets of supersaturated ammonium nitrate solution, coated with emulsifier/oil phase, ranges from 2 to 10 μm. The smallest represent separate droplets, whereas larger are most probably agglomerates.

A comparison of both dynamic TG curves of sample 1 (consists of water, AN, oil phase and emulsifier) and sample 2 (contains also a certain amount of SN) is shown in Figure 4. From room temperature up to around 150 ^{o}C only water is released from the samples (see Figure 5B). At a heating rate of 5 K min^{-1} there is no clear plateau between dehydration and thermal decomposition of AN and oil phase. Better resolution between these two processes could be obtained with a lower heating rate, but even at a heating rate of 0.4 K min^{-1} we could not clearly separate the first weight loss from the second. After dehydration, decomposition of AN and oil phase takes place according to the idealized reaction: $3n\ NH_4NO_3 + (CH_2)_n \rightarrow n\ CO_2 + 7n\ H_2O + 3n\ N_2$ [7]. Evolved gas analysis (TG-MS), shown in Figure 5A, enables to detect all of these gasses (mass peaks 44 corresponds to CO_2, 18 to H_2O and 28 to N_2). Besides, CO (mass peak 28 coincides for N_2 and CO evolution, but mass peaks 29 and 16 with small intensity confirm the presence of CO), NO (mass peak 30) and NO_2 (mass peak 46) were detected, meaning that decomposition reaction is far more complex than idealized reaction.

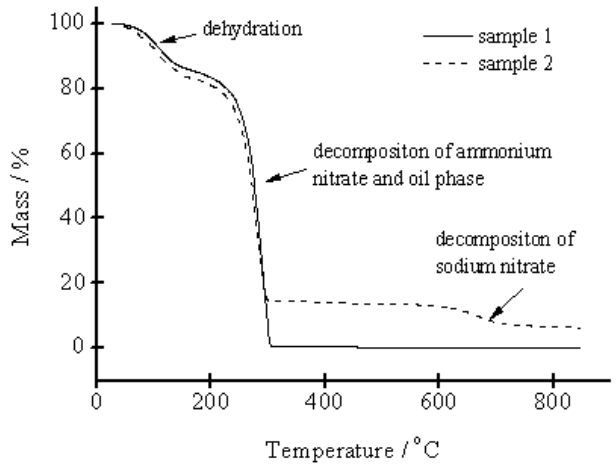

Figure 4. Comparison of dynamic thermogravimetric curves of samples 1 and 2.

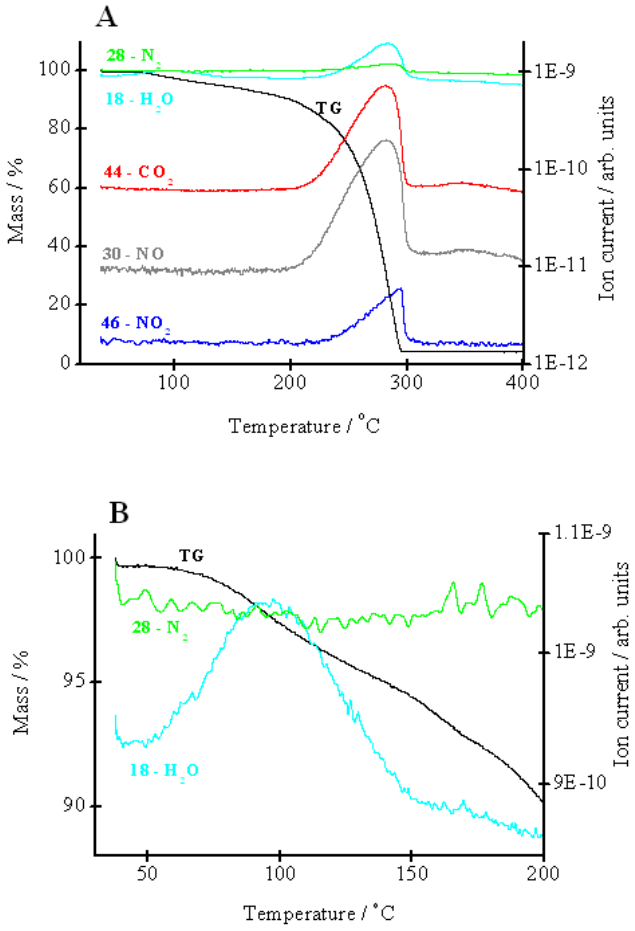

Figure 5. TG-MS curves of sample 1. Figure5A represents a whole temperature range while in Figure 5B magnification within the temperature range from 30 to 200 °C is shown.

From the difference of the weight loss at 310 °C and water content, the sum of AN, oil content and emulsifier can be calculated. The total weight loss at 310 °C is 100 % for sample 1 (Figure 4). Sample 2 displays another weight loss (onset temperature approximately 610 °C) due to thermal decomposition of SN [28]. In Figure 6A dynamic TG curve of a pure (99.999 %) SN is represented. Onset and endset temperatures of its thermal decomposition are 600 and 800 °C. The calculated weigh loss of 53.7 % confirms that solid residue is sodium peroxide Na_2O_2 (theoretical weight loss 54.1. %) [29], rather than to Na_2O (theoretical weight loss in that case would be 63.5 %). From Figure 6B it is evident that SN starts to decompose already below 400 °C.

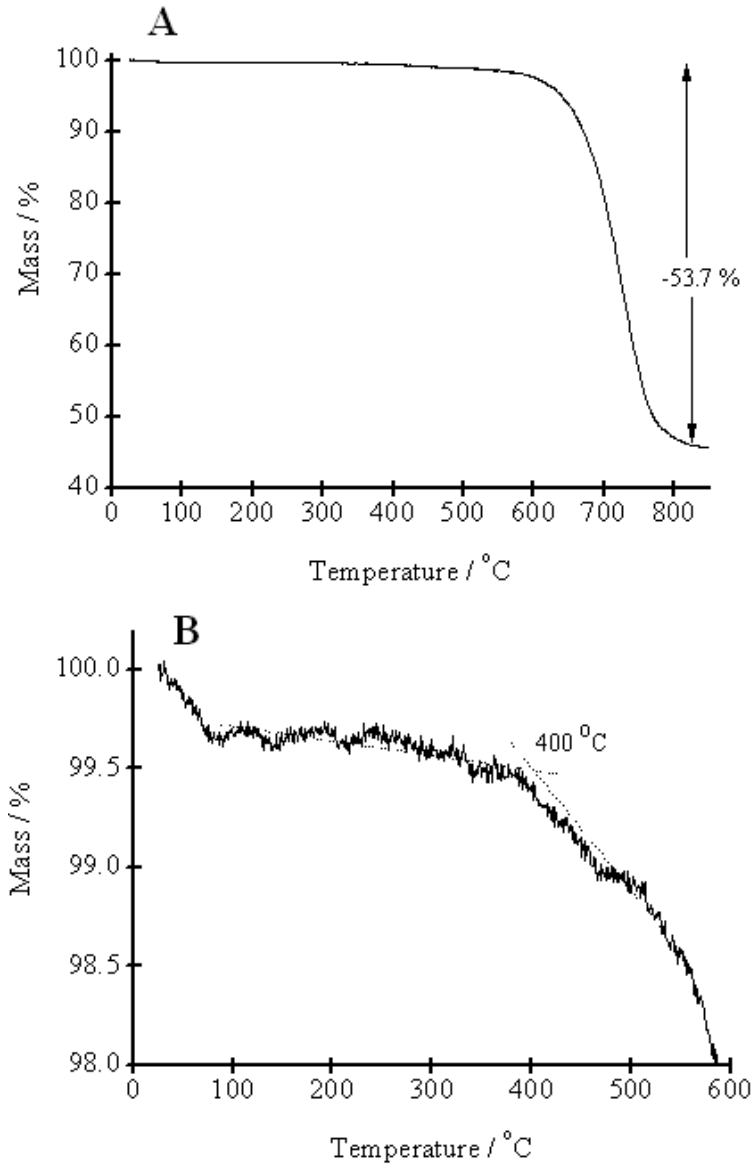

Figure 6. TG curve of $NaNO_3$ obtained under an air atmosphere (A). Initial mass of the sample was around 3.8 mg. The magnification of the temperature range from 25 to 600 °C is shown in Figure B.

Measurement of maximal resolution ("maxres") of sample 1 is shown in Figure 7. Under the specific temperature programme (described in 4th paragraph of Experimental) it is possible to separate the dehydration process from the beginning of thermal decomposition of AN and the organic phase. Unfortunately, since the temperature program regulates itself within the preset parameters on the basis of a DTG curve (the rate of weight loss), we could not subtract a blank curve and therefore the weight loss due to dehydration, as well for the decomposition process, is not accurate. However, this measurement helps us to determine the isothermal temperature at which probably all the water would leave the sample (100 ^{o}C – see Figure 7B). The isothermal TG curves of both samples are shown in Figure 8. The time needed for dehydration depends strongly on the mass of sample. In the case of sample 2 the signal stabilized after 180 min (weight loss 15.5 %), whereas for sample 1 after 5 hours (13.5 % weight loss). From the isothermal weight loss at 100 ^{o}C the water content in both samples was determined.

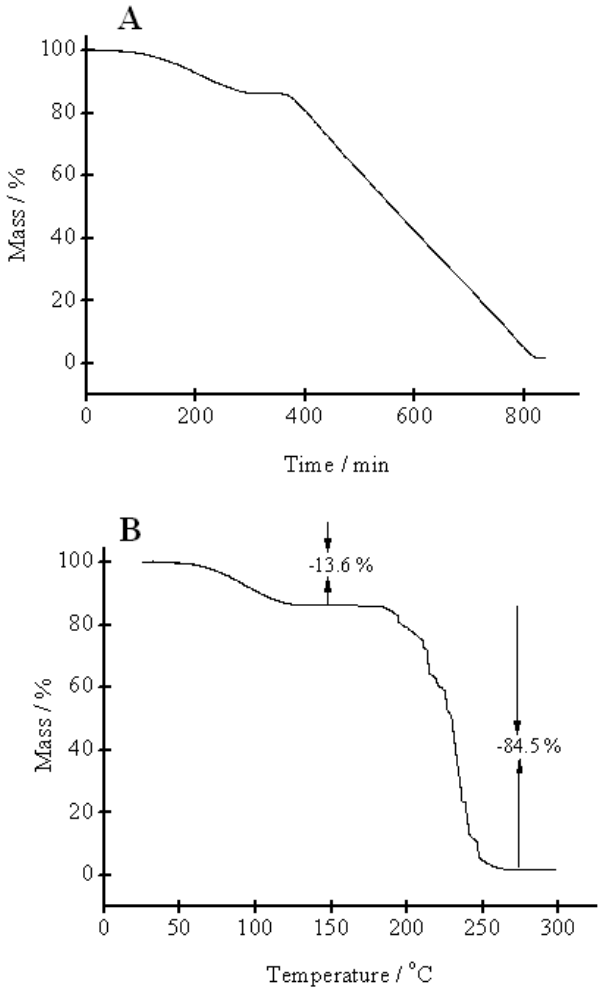

Figure 7. Original "maxres" measurement of sample 1 took 14 hours (A). Figure B represents the same curve, plotted versus temperature. The sample was placed in a 40 μL aluminum crucible and covered with 50 μm perforated lid.

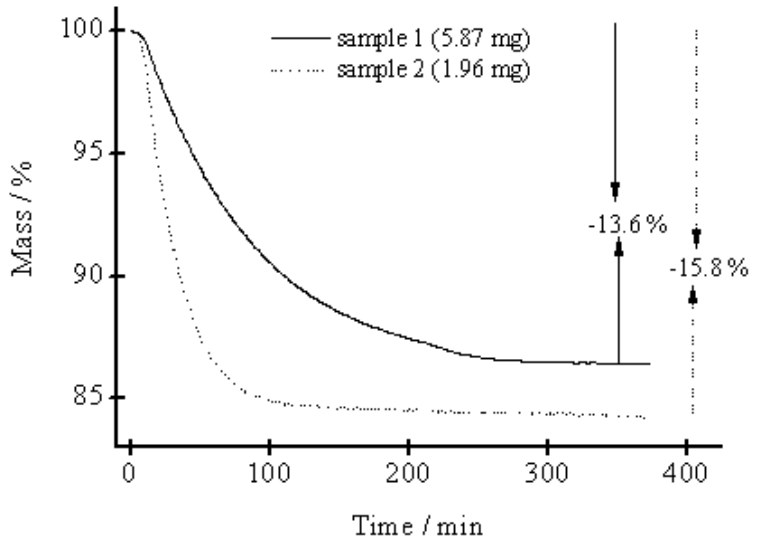

Figure 8. Isothermal TG measurement, performed at 100 °C. The final temperature in the furnace was reached after 15 minutes.

AN has been well studied since it undergoes at least two phase transitions from room temperature until it melts at 169 °C (Figure 9) [8, 30, 31]. The transition temperatures, especially from the IV → III and IV → II state, depend on several factors, especially on the thermal history of the sample and on the water and impurity content [8, 30–33]. The water content is recognized to be responsible for the phase transition IV → III, as well for the wide temperature range within which this transition occurs [30, 31]. The peak at 126 °C (II → I) is not affected by the conditions and is well reproducible as regards both, enthalpy and temperature [30]. Several values were published for the enthalpy of this phase transformation, ranging from 51.2 to 63 J g^{-1}.

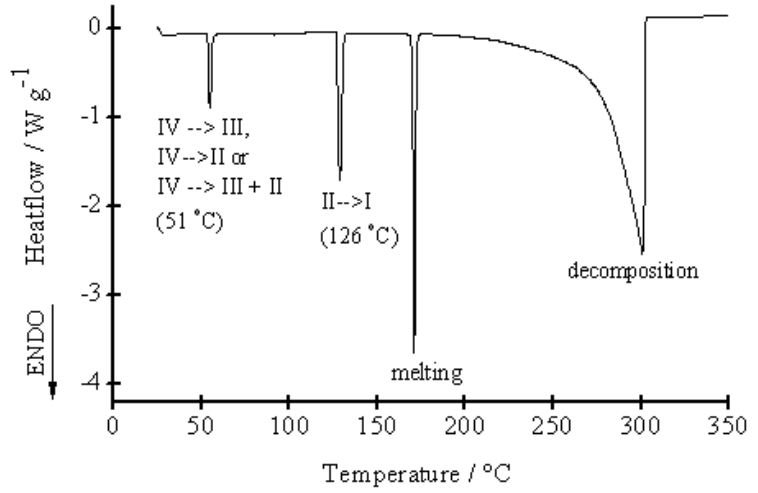

Figure 9. DSC curve of dried AN.

We performed several successive heating and cooling measurements (cycling experiments) on pure dried AN from 25 up to 135 °C. The value obtained in the 1st cycle was smaller than in 2nd, in all cases regardless the measuring conditions (Table 1). Using a pierced lid, the value slowly started to decrease. From the 2nd to 5th cycle the value decreased by approximately 0.3 %. This phenomenon was more distinct when we used opened pans, when the value from the 2nd to 5th cycle diminished by 3.0 %. Therefore the corresponding TG measurements were performed (with the same temperature programme, same type of crucibles and lids) on the same sample. From Figure 10 it is evident that the weight in the case of a pierced lid and without a lid decreases with time, which means that at that temperature AN has a considerable vapour pressure. From the 1st up to the 5th cycle the weight loss was 0.5 % (pierced lid) or 3.8 % when an open pan was used. Measured weight losses are in accordance with the observations made during DSC cycling experiments. In the case of a 50 μm perforated lid, the signal on the TG and DSC curve remained stable for several cycles, with ΔH = 55.20 ± 0.20 J g^{-1} (average value of ten cycling experiments; for each a mean value from the second to tenth heating scan was taken). This value is very close to the value published already in 1967 (ΔH = 55.41 ± 0.38 J g^{-1}) [34].

Table 1. Values of the enthalpies in J g^{-1} for the phase transition at 126 °C of a pure AN in open pan, pan covered with a pierced lid or 50 μm perforated lid

Cycle no.	Open pan	Pierced lid	Perforated lid
1	54.83	54.80	55.16
2	54.88	54.87	55.21
3	54.32	54.83	55.19
4	53.76	54.78	55.22
5	53.21	54.69	55.20

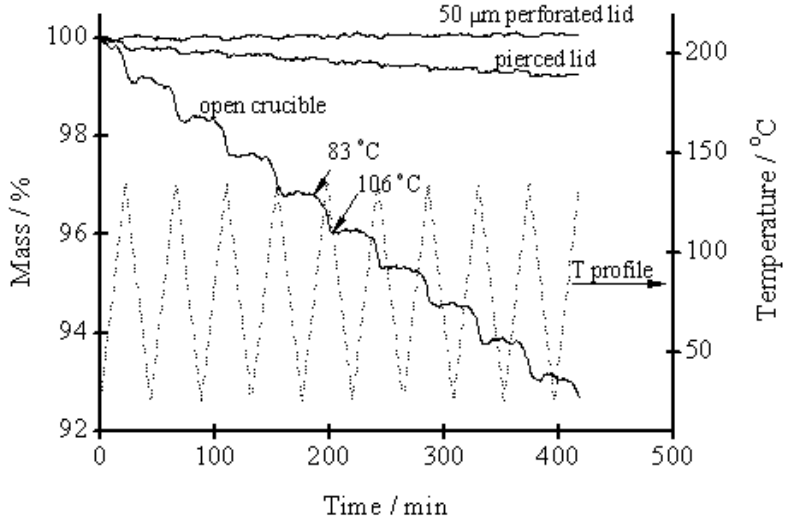

Figure 10. Successive heating and cooling TG experiment (10 cycles) of dry AN in an open crucible, in a crucible covered with a manually pierced lid and with 50 μm perforated lid.

In the emulsion AN is present as an amorphous component. Cycling of the emulsion transforms amorphous AN to the crystallinic form (Figure 11). In the 1st cycle no peaks are observed on heating. In the second the basic shapes of the peaks are formed. On heating the peak at 126 °C reaches a stable value after several cycles, which is then used to calculate the amount of AN in the sample by simply dividing ΔH (sample) / ΔH (AN standard).The estimated error in this determination is ± 0.7 %. As for pure AN, it is necessary to perform cycling in pans covered with perforated lids for the same reasons as already described above. With the help of the corresponding TG experiments we observed that AN in emulsion starts to crystallize only when water is released from the sample. Dehydration must be complete, and after it an additional four or five cycles are necessary that AN completely crystallize (Figure 12, Table 2). Dehydration occurs earlier in the case open pans or pans covered with a pierced lid are used. This means that the peak at 126 °C reaches its maximum value within a smaller numbers of cycles, but the value is not correct since some AN has already evaporated by that time when a stable value was reached. In hermetically sealed pans, no peaks are observed in the cycling experiment within this temperature range.

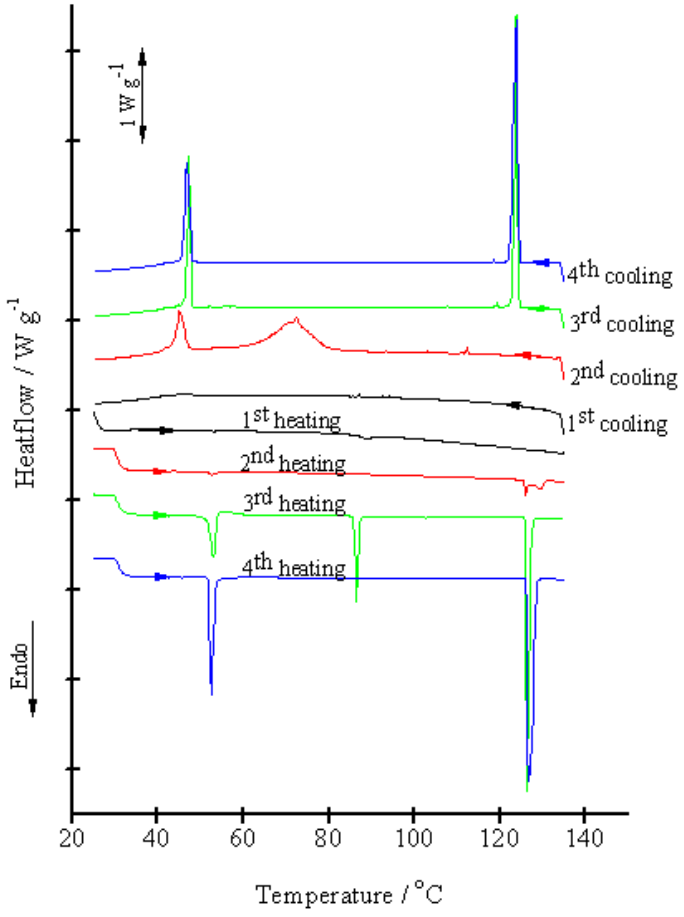

Figure 11. DSC cycling experiment of sample 1 (50 µm perforated lid). On repeated scans AN begins to crystallize.

Table 2. Calculated content of AN in sample 1 [in %] in differently covered pans. Values from the third cycle up to the tenth are given

Cycle no.	Open pan	Pierced lid	Perforated lid
3	73.1	75.6	59.5
4	71.9	77.8	74.1
5	70.6	78.4	78.2
6	68.8	78.1	79.2
7	67.5	77.8	79.3
8	66.2	77.4	79.5
9	64.9	77.0	79.5
10	63.8	76.7	79.5

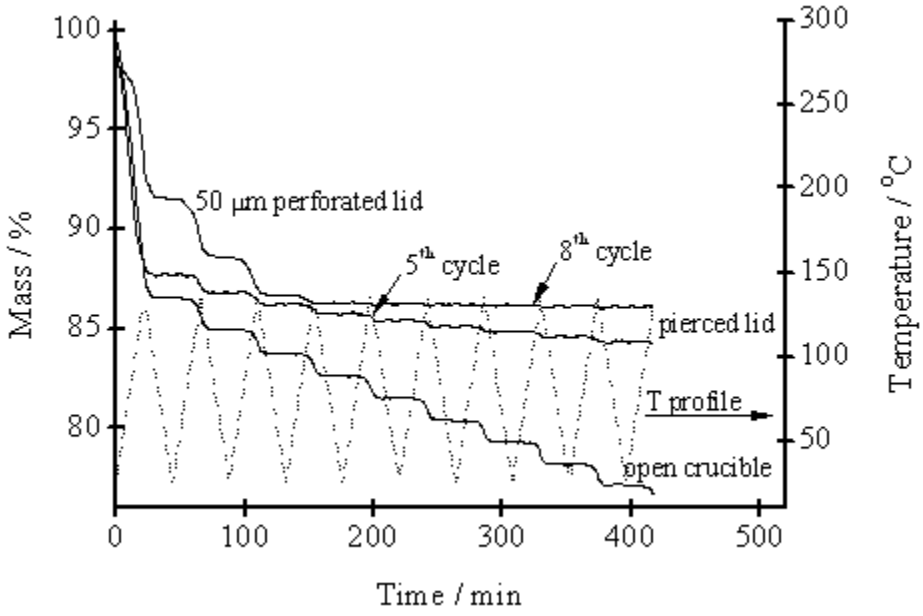

Figure 12. TG cycling experiment (10 heating and cooling cycles) of sample 1. During the 8th cycle the ΔH value for the phase transition at 126 ^{o}C reaches its maximum value on the DSC curve and then remains constant up to several tens of cycles. When the pan was covered with a pierced lid, the maximum was obtained in the 5th cycle, but ΔH was smaller and then continuously decreased (Table 2).

Using the DSC measurement described, it was impossible to analyze sample 2, which besides AN contains also SN as oxidizing agents. Figure 13 shows a DSC curve of sample 2, which was previously 9 times cycled between 25 and 135 ^{o}C. AN is already crystallized, but its content could not be determined, because in a mixture with SN an eutectic system is formed [35]. Eutectic composition melts (at 120.8 ^{o}C) close before a phase transition from tetragonal to cubic crystalline modification at 126 ^{o}C takes place. The peak which still occurs at that temperature corresponds to the transition of the unmelt AN. On further heating, the rest of the solid AN melts. Temperature where a DSC curve again reaches the baseline

corresponds to the liquidus curve of the AN/NN composition in water phase. For the already crystallized sample 2 the final temperature of the melting was 142 °C.

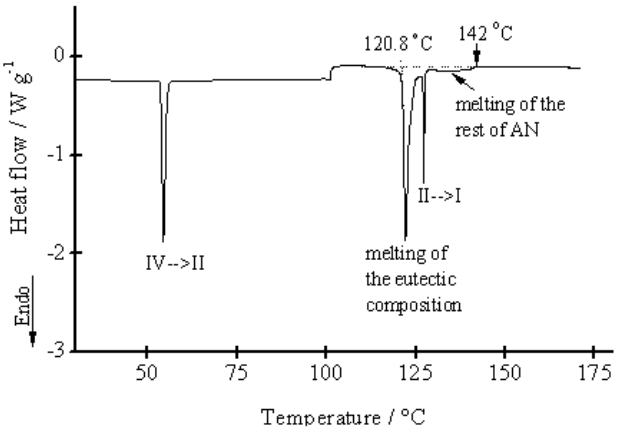

Figure 13. DSC curve of sample 2, previously cycled 9 times from 25 to 135 ° C. From 25 to 100 °C the heating rate was 5 K min^{-1} and from 100 to 170 °C 2 K min^{-1}.

In diethyl ether both inorganic salts (AN and NN) are insoluble, whereas organic matter readily dissolves. Using this solvent, quantitative separation of both salts is therefore possible from sample 2. On the basis of both TG curves of sample 2 (original sample and inorganic precipitate which remained after separation – see Figure 14A, B) the weigh percent of ammonium nitrate in sample 2 was calculated using the following equation:

$$\frac{\omega(AN)_{sample}}{\omega(SN)_{sample}} = \frac{\omega(AN)_{separation}}{\omega(SN)_{separation}}$$

$$\omega(AN)_{sample} = \frac{82.6\% \cdot 13.7\%}{17.4\%} = 65.0\%$$

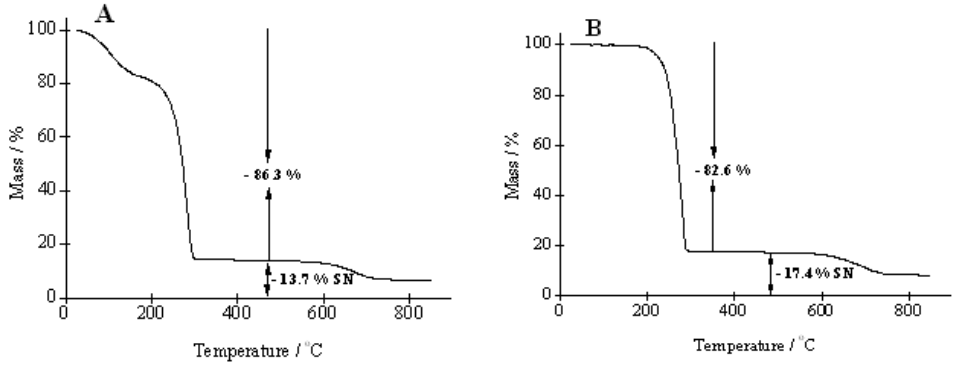

Figure 14. Dynamic TG measurement of original sample 2 – A, and inorganic precipitate obtained after separation of the same sample from diethyl ether – B.

In sample 2 the whole weight that remains after dehydration and thermal decomposition of AN and organic components is attributed to the SN content (Figure 14A). SN content should be carefully read from TG curve. Taking into account that thermal decomposition of SN begins before 400 °C (see Figure 6B), the value around 370 °C should be taken. But under closer inspection of a TG curve of original sample 2, a weight loss of around 1 % is observed in a temperature range form 300 to 470 °C (a long tail), which we attributed to thermal decomposition of emulsifier; therefore the mass of SN at 470 °C was taken for calculation. After separation in diethyl ether the weight loss up to 300 °C is smaller and is attributed only to thermal decomposition of AN (Figure 14B).

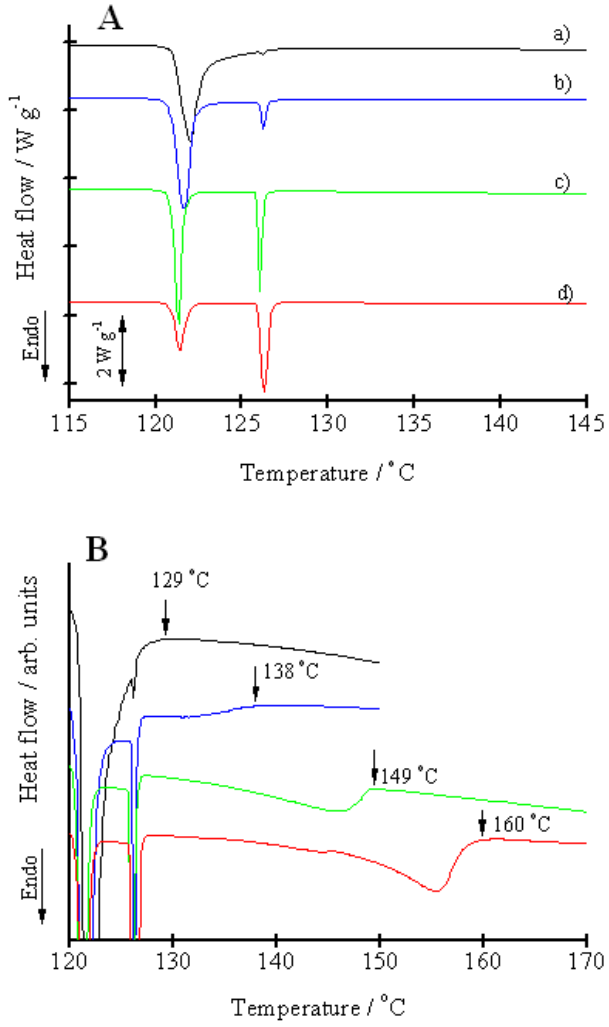

Figure 15. Heating DSC curves obtained for different AN/NN compositions (A). The content of AN increases from a) to d) and therefore the intensity of the peaks, correspond to the melting of the eutectic composition (120.8 °C) decreases whereas those of the II to I solid transition of the AN (126 °C) increases. The magnification of the investigated region is shown in Figure B.

The error in determination of the AN content can be very large. For instance, a 0.5 % lower value for the amount of ω(NN) in sample 2 (13.2.% - Figure 14A) and a 0.5 % lower

value for AN content in the precipitate (82.1 % - Figure14B) give as a result 60.5 % of AN in the sample (± 4.5 %). If both differences are 0.3 %, the calculated result is 62.3 % (± 2.7 %). To avoid such a large error, at least five measurements should be performed after making sure that no systematic error is present in the determination.

To avoid time consuming separation procedure of both salts from an emulsion, a part of a binary phase diagram of AN/NN was constructed. On the basis of the TG results (82.6 % AN in a binary mixute with NN), AN/NN mixtures with a weight % of AN from approximately 74 to 92 % were prepared by carefully weighing both salts. DSC curves of these samples were measured with a heating rate of 2 K/min (Figure 15A) and the final melting temperatures of the solid AN (which rests after melting of eutectic composition) were determined. The magnification of the investigated temperature region is shown in Figure 15 B. From these data a liquidus curve of the AN rich part of a phase diagram was constructed (Figure 16).

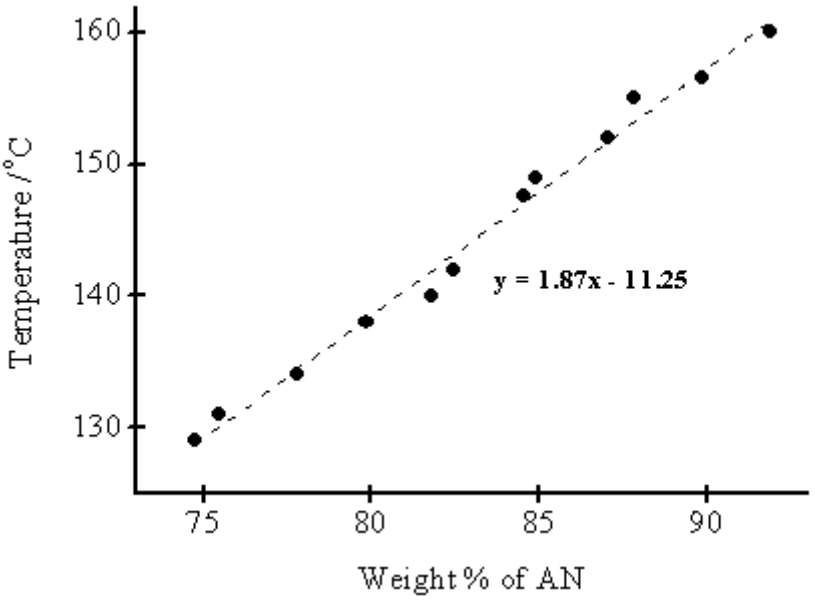

Figure 16. A part of a liquidus curve, determined for the AN rich side of the AN/NN phase diagram.

Weigh percent of AN in sample 2, where AN and NN already crystallized (Figure 13), can now be calculated from the linear relationship between composition and final melting temperature of AN (142 ^{o}C). The obtained value is 81.9 % AN; the difference from 100 % corresponds to SN, i.e. 18.1 %. The weight percent of AN in sample 2 can be calculated as follows:

$$\frac{\omega(AN)_{sample}}{\omega(SN)_{sample}} = \frac{\omega(AN)_{water.phase}}{\omega(SN)_{water.phase}}$$

$$\omega(AN)_{sample} = \frac{81.9\% \cdot 13.7\%}{18.1\%} = 61.9\%$$

Content of SN in the original sample is still needed (see Figure 14A). Using this method, the final value of the AN content in sample 2 is 61.9 %. In the case where the final melting point deviates for ± 1 ^{o} and SN content in the original sample for ± 0.5 %, the uncertainty for AN content is still ± 2 %. However, once the required part of the phase diagram is constructed, the last described method would be much less time consuming in the case of serial measurements.

CONCLUSION

Thermal methods of analysis (TG and DSC) proved to be suitable methods to determine water content and the amount of AN, SN and organic phase in water-in-oil emulsions. Water content was determined by isothermal TG measurement at 100 ^{o}C. In sample 1 the amount of AN was determined by performing ten heating and cooling DSC cycles between 25 and 135 ^{o}C. During this experiment, water evaporated and AN began to crystallize. From the enthalpy of the phase transition at 126 ^{o}C the amount of AN was calculated. The content of organic phase (oil + emulsifier) was calculated from the difference from 100 %.

Amount of water, AN, SN and organic phase in sample 1 and 2 are as follows:

	Sample 1	Sample 2
water	13.6 %	15.8 %
AN	79.5 %	65.0 (61.9)%
SN	/	13.7 %
organic phase	6.9 %	5.5 (8.6)%

The values in parenthesis (for sample 2) represent the content of AN calculated from an AN/NN phase diagram. Consequently the content of organic phase is also different.

In sample 2 the amount of SN corresponded to the weight remaining at 470 ^{o}C in dynamic TG measurement. AN content was calculated on the basis of an equation which assumes that the ratio of AN and SN in sample 2 is equal to that in a quantitatively obtained salt precipitate from diethyl ether, where organic compounds remain in solution. Again, the difference from 100 % is attributed to the sum of hydrocarbon oil and emulsifier.

Unknown ratio between AN/SN in an emulsion was also determined from the liquidus curve of the binary phase diagram, a part of which was constructed for this purpose. In that case separation from organic matter was not necessary. Approximately 3 % lower value for AN content was determined with the latter method (61.9 %). We ascribed the observed discrepancy to the fact that most probably a small amount of organic phase still remained in an inorganic precipitate after separation. Therefore a weight loss from 25 to 300 ^{o}C was larger.

REFERENCES

[1] Hemminger, W.; Sarge, S. M. In *Handbook of Thermal Analysis and Calorimetry*; Brown M. E.; Ed.; Principles and Practice; Elsevier: Amsterdam, NL, 1998; Vol.1, pp 7-9.

[2] Leskelä, T.; Thermoanalytical Techniques in The Study of Inorganic Materials, Dissertation; Helsinki University of Technology, Helsinki, FI, 1996; pp 7-50.

[3] Norem, S.D.; O'Neill, M. J.; Gray, A. P. *Thermochim. Acta*, 1970, 1, 29-38.

[4] McGhie, A. R.; Chiu, J., Fair, P. G.; Blaine, R. L. *Thermochim. Acta*, 1983, 67, 241-250.

[5] Wendlandt, W. W. *Thermal Analysis*; 3rd Ed.; Wiley, New York, US, 1986; p.461.

[6] Mullens, J. In *Handbook of Thermal Analysis and Calorimetry*; Brown M. E.; Ed.; Principles and Practice; Elsevier: Amsterdam, NL, 1998; Vol.1, p 509

[7] Bampfield, H. A.; Cooper, J. In *Encyclopedia of Emulsion Technology*; Becher, P.; Ed.; Applications; Marcel Dekker Inc.: New York, US, 1988; Vol. 3, pp. 282 - 306.

[8] Oommen, C.; Jain, S. R. *J. Hazard. Mater*. 1999, A67, 253-281.

[9] Klapotke, T. M.; Sabate, C. M.; Rusan, M. Z. *Anorg. Allg. Chem*. 2008, 634, 688-695.

[10] Long, G. T.; Wight, C. A. *J. Phys. Chem*. 2002, 106, 2791-2795.

[11] Zeman, S.; Gazda, Š.; Štolceva, A.; Drab, J. *Thermochim. Acta* 1993, 230, 177-189.

[12] Zeman, S. *Thermochim. Acta*, 1993, 230, 191-206.

[13] Yang, G. C.; Nie, F. D.; Huang, H.; Zhao, L.; Pang, W. T. *PropellantsExplos.Pyrotech*. 2006, 31, 390-394.

[14] Talawa,r M. B.; Sivabalan, R.; Senthilkumar, N.; Prabhu, G.; Asthana, S. N. *J. Hazard. Mater*. 2004, 113, 13-27.

[15] de Klerk, W. P. C.; Popescu, C.; van der Heijden, A. E. D. M. J. *Therm. Anal.Cal*. 2003, 72, 955-966.

[16] Simões, P. N.; Pedroso, L. M.; Portugal, A. A.; Campos, J. L. *Thermochim. Acta*, 1998, 319, 55-65.

[17] Lee, J.S.; Hsu, C. K.; Chang, C. L. *Thermochim Acta*, 2002, 392, 173-176.

[18] Jones, D. E. G.; Lightfoot, P. D.; Fouchard, R. D.; Kwork, Q.; Turcotte, A. M.; Ridley, W. *Thermochim. Acta*, 2002, 384, 57-69.

[19] Plato, C.; Glasgow, A. R. *Anal. Chem*. 1969, 41, 330-336.

[20] Sućeska, M.; Rajić M. *Proc. of 31st International Annual Conference of ICT*; (Ed) Fraunhofer Institet für Chemishe Technologie; Karlsruhe, Germany, June 27 - 30, 2000; pp. 84/1 – 84/15

[21] Weese, R. K.; Burnham, A. K.; Turner, H. C.; Tran, T. D. *J.Therm. Anal. Cal*. 2007, 89, 465-473.

[22] Lee, J. S.; Jaw, K. S. *J.Therm. Anal. Ca*l. 2006, 85, 463-467.

[23] Oxley, J. C.; Kaushik, S. M.; Gilson, N. S. *Thermochim. Acta*, 1992, 212, 77-85.

[24] Oxley, J. C.; Smith, J. L.; Wang, W. *J. Phys. Chem*. 1994, 98, 3893-3900.

[25] Lightfoot, P. D.; Fouchard, R. C.; Turcotte, A.-M.; Kwork, Q. S. M.; Jones, D. E. G. *Journal of Pyrotechnics*, 2001, Issue 14, 15- 26

[26] Burns, D.T.; Lewis, R. J.; Bridges, J. *Anal. Chim. Acta*, 1998, 375, 255-260

[27] Cerc Korošec, R.; Kajič, P.; Bukovec, P. *J.Therm. Anal. Cal*. 2007, 89, 619-624.

[28] Sweeney, M.; *Thermochim. Acta*, 1975, 11, 409-424.

[29] Kramer, C. M.; Munir, Z. A.; Volponi, J. V. *J.Therm. Anal*. 1983, 27, 410-408.
[30] Dellien, I. Thermochim. acta, 1982, 55, 181 191.
[31] Siemões, P. N.; Pedroso, L. M.; Portugal, A. A.; Campos, J. L. *Thermochim. Acta*, 1998, 319, 55-65.
[32] Kim, J. H. *J. Chem. Eng. Japan*, 1997, 30, 336-338.
[33] Ingman, J. S.; Kearley, G. J.; Kettle, F. A. *J. Chem. Soc. - Faraday Trans*. 1982, 178, 1817-1826.
[34] Nagatani, M.; Seiyama, T.; Sakiyama, M.; Suga, H.; Seki, S. *Bull. Chem. Soc. Jpn*. 1967, 40, 1833-1844.
[35] Early, R. G.; Lowry, T. M. *J. Chem. Soc*. 1922, 121, 963-.